



AALBORG UNIVERSITY
DENMARK

Aalborg Universitet

A Double Phase-Shift Control Strategy for A Full-Bridge Three-Level DC/DC Converter

Liu, Dong; Deng, Fujin; Gong, Zheng; Chen, Zhe

Published in:

Proceeding of The 42nd Annual Conference of IEEE Industrial Electronics Society, IECON

DOI (link to publication from Publisher):

[10.1109/IECON.2016.7793214](https://doi.org/10.1109/IECON.2016.7793214)

Publication date:

2016

Document Version

Accepted author manuscript, peer reviewed version

[Link to publication from Aalborg University](#)

Citation for published version (APA):

Liu, D., Deng, F., Gong, Z., & Chen, Z. (2016). A Double Phase-Shift Control Strategy for A Full-Bridge Three-Level DC/DC Converter. In *Proceeding of The 42nd Annual Conference of IEEE Industrial Electronics Society, IECON* (pp. 1202 - 1207). IEEE Press. <https://doi.org/10.1109/IECON.2016.7793214>

General rights

Copyright and moral rights for the publications made accessible in the public portal are retained by the authors and/or other copyright owners and it is a condition of accessing publications that users recognise and abide by the legal requirements associated with these rights.

- Users may download and print one copy of any publication from the public portal for the purpose of private study or research.
- You may not further distribute the material or use it for any profit-making activity or commercial gain
- You may freely distribute the URL identifying the publication in the public portal -

Take down policy

If you believe that this document breaches copyright please contact us at vbn@aub.aau.dk providing details, and we will remove access to the work immediately and investigate your claim.

A Double Phase-Shift Control Strategy for A Full-Bridge Three-Level DC/DC Converter

Dong Liu, Fujin Deng, Zhe Chen

Department of Energy Technology

Aalborg University

Aalborg, Denmark

dli@et.aau.dk, fde@et.aau.dk, zch@et.aau.dk

Abstract—In this paper, a double phase-shift control strategy is proposed for a full-bridge three-level (FBTL) dc/dc converter in dc distribution systems with the medium dc bus voltage. The proposed control strategy can effectively reduce the voltage change rate dv/dt and voltage stress on the transformer, which means that the reliability and EMC of the FBTL dc/dc converter can be improved. The operation principle and performances of the proposed control strategy is analyzed in detail. Finally, the simulation results are presented to verify the proposed control strategy.

Keywords—Full-bridge; medium dc bus voltage; phase-shift; three-level dc/dc converter.

I. INTRODUCTION

Dc distribution systems and dc micro-grids have been proposed as promising solutions for future smart-grid systems because of their clear merits, such as no reactive power, no frequency stability, high conversion efficiency, and easy system control [1-3]. Furthermore, dc-based data centers and residential systems have been increasingly developed recently [4], [5]. The performance of dc systems highly depends on dc/dc converters, which are responsible for delivering power and changing voltage levels in dc grids. Generally, a high or medium dc voltage is needed for the dc distribution systems and micro-grids to reduce the transmission losses and increase the power delivery capability. Therefore, the scientific researches on the medium voltage dc/dc converters with high performance and high reliability are quite desired.

The three-level (TL) dc/dc converter is attractive for the dc distribution grids with the medium dc bus voltage [6]. So far, a number of studies have been done on TL based dc/dc converters [7-15]. In [7], a zero voltage and zero current switching half-bridge (HB) TL dc/dc converter was proposed, in which a flying capacitor in the primary side is added to make the phase-shift control strategy applied to TL dc/dc converter. Based on [7], an auxiliary circuit is added in the secondary side to reduce the circulating current for improving the efficiency [8]. In [9], a new four-switch HB zero-voltage-switching (ZVS) TL dc/dc converter was proposed, which features with simple and compact circuit structure by adding one additional wire between the mid-points of the input capacitors and switching pairs but removing two clamped diodes. The new solutions to achieve the wide range soft-

switching are discussed in [10] based on the circuit structure of the four-switch HBTL converter, in which four kinds of new pulse-wide modulation PWM TL dc/dc converters are proposed for the industrial application. A secondary-side phase-shift-controlled ZVS dc/dc converter with wide voltage gain and a three-phase dc/dc converter with low voltage stress on the power switches are proposed in [11] and [12] for the high voltage applications. Two control strategies which are chopping phase-shift (CPS) control and double phase-shift (DPS) control respectively are presented in [13] and [14] for the isolated full-bridge three-level (FBTL) dc/dc converter. But the two control strategies both cause high voltage change rate dv/dt on the primary side voltage of the transformer, which would cause large electromagnetic interference (EMI) and thus lead them not suitable for the medium or high voltage applications. In [15], an improved FBTL dc/dc converter with a voltage balance control strategy of the input capacitors is proposed to reduce the dv/dt . However, a passive filter is inserted into the primary side of the transformer, which would result in reducing the voltage conversion rate and efficiency.

In this paper, a double phase-shift control strategy is proposed for the FBTL dc/dc converter applied to the dc grids with the medium dc bus voltage. Comparing with the conventional control strategy, the proposed control strategy can effectively reduce the voltage change rate dv/dt and voltage stress on the transformer, and thus improve both EMI and reliability of the converter. The operation principle and performance of the proposed control strategy are analyzed in detail. Finally, the simulation results are shown to validate the proposed double phase-shift control strategy.

This paper is organized as follows. Section II analyzes the operation principle of the proposed double phase-shift control strategy in detail. Section III analyzes the characteristics and performances of the FBTL dc/dc converter under the proposed control strategy theoretically. Section IV presents the simulation results to verify the theoretical analysis. Finally, the main contributions of this paper are summarized in Section V.

II. OPERATION PRINCIPLE

Fig. 1 shows the circuit structure of the FBTL dc/dc converter and main operation waveforms under the proposed double phase-shift control strategy. C_{i1} and C_{i2} are two input capacitors which split the input voltage V_{in} into V_1 and V_2 . S_1 -

S_8 and D_1 - D_8 are power switches and their body diodes. C_1 - C_8 are junction capacitors. C_{s1} and C_{s2} are two flying capacitors. D_9 - D_{12} are four clamped diodes. L_r is leakage inductance of the transformer T_r . In the secondary side, there are four rectifier diodes D_{r1} - D_{r4} , an output filter L_o , and an output filter capacitor C_o . In Fig. 1(a), the input voltage is V_{in} ; the voltage between point a and b is V_{ab} ; the primary current of the transformer is i_p ; the current through output filter inductor is i_{Lo} ; the output current and voltage are I_o and V_o ; the turns ratio of the transformer T_r is n . In Fig. 1(b), d_{rv1} - d_{rv8} are driving signals of the switches S_1 - S_8 ; α_1 and α_2 are two time delays.

For simplifying the analysis, some assumptions are made: 1) all the capacitors and inductances are ideal; 2) all the power devices and the diodes are ideal; 3) the power switches S_1 - S_8 have the same parasitic capacitors, which means that $C_1 = C_2 = C_3 = C_4 = C_5 = C_6 = C_7 = C_8 = C_j$; 4) the input divided capacitors C_{i1} and C_{i2} are large enough to be regarded as two voltage sources with the value of $V_{in}/2$; 5) the two flying capacitors C_{s1} and C_{s2} are large enough to be regarded as two voltage sources with the values of $V_{in}/2$; and 6) the output filter inductance L_o is large enough to be regarded as a constant current source during a switching period.

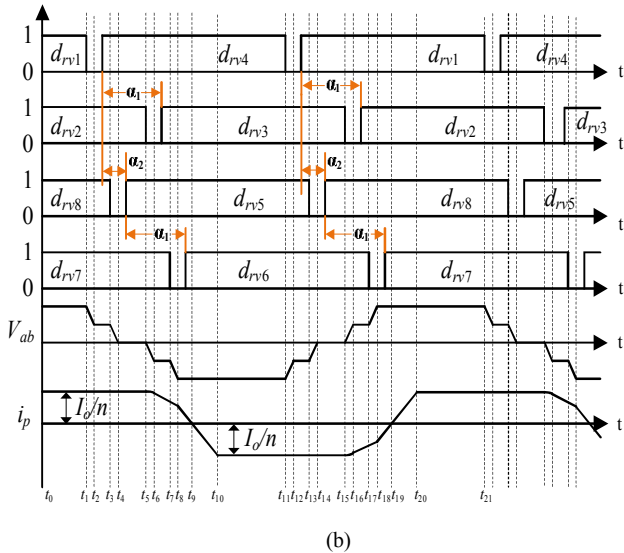
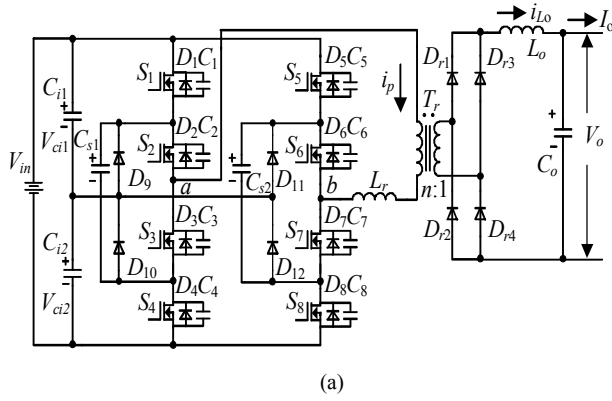


Fig. 1. Circuit structure and main operation waveforms. (a) Circuit Structure. (b) Main waveforms under the proposed control strategy

Fig. 2 shows the equivalent circuits under the proposed double phase-shift control strategy.

Stage 1 [$t_0 - t_1$]: During this period, S_1 , S_2 , S_7 , and S_8 are all on-state, so V_{ab} equals V_{in} and the input power transfers to the load from D_{r1} and D_{r4} . During this stage, the primary current of the transformer i_p is I_o/n .

Stage 2 [$t_1 - t_2$]: At t_1 , S_1 is turned off. Then I_o is reflected to the primary side, which means i_p is still I_o/n to charge C_1 and discharge C_4 via C_{s1} . Therefore, V_{c1} increases and V_{c4} decreases linearly.

$$V_{c1}(t) = \frac{I_o}{2 \cdot n \cdot C_j} (t - t_1) \quad (1)$$

$$V_{c4}(t) = \frac{V_{in}}{2} - \frac{I_o}{2 \cdot n \cdot C_j} (t - t_1) \quad (2)$$

The duration of the stage 2 is:

$$t_2 - t_1 = \frac{n \cdot V_{in} \cdot C_j}{I_o} \quad (3)$$

Stage 3 [$t_2 - t_3$]: At t_2 , V_{c1} increases to $V_{in}/2$ and D_9 conducts, which clamps V_{c4} at 0 V. Therefore, S_4 can be turned on with zero-voltage. During this stage, V_{ab} is $V_{in}/2$ and i_p remains I_o/n .

Stage 4 [$t_3 - t_4$]: At t_3 , S_8 is turned off; i_p maintains at I_o/n to charge C_8 and discharge C_5 via C_{s2} . V_{c8} increases and V_{c5} decreases linearly.

$$V_{c8}(t) = \frac{I_o}{2 \cdot n \cdot C_j} (t - t_3) \quad (4)$$

$$V_{c5}(t) = \frac{V_{in}}{2} - \frac{I_o}{2 \cdot n \cdot C_j} (t - t_3) \quad (5)$$

The duration of the stage 4 is

$$t_4 - t_3 = \frac{n \cdot V_{in} \cdot C_j}{I_o} \quad (6)$$

Stage 5 [$t_4 - t_5$]: At t_4 , V_{c8} increases to $V_{in}/2$ and D_{12} conducts, which clamps the voltages of S_5 at 0 V. So S_5 can be turned on with zero-voltage. During this stage, V_{ab} is 0 V and i_p is I_o/n .

Stage 6 [$t_5 - t_6$]: At t_5 , S_2 is turned off. Then C_2 is charged and C_3 is discharged; V_{ab} changes to negative. The current i_p starts to decrease and is not enough to provide I_o , so D_{r1} , D_{r2} , D_{r3} , and D_{r4} conduct simultaneously, which clamps both the primary and secondary voltage at 0 V. Thus the voltage of V_{ab} is fully applied on L_r . During this stage, L_r resonates with C_2 and C_3 .

$$i_p(t) = \frac{I_o}{n} \cdot \cos \omega_r (t - t_5) \quad (7)$$

$$V_{c2}(t) = \frac{I_o}{n} \cdot Z_r \cdot \sin \omega_r (t - t_5) \quad (8)$$

$$V_{c3}(t) = \frac{V_{in}}{2} - \frac{I_o}{n} \cdot Z_r \cdot \sin \omega_r (t - t_5) \quad (9)$$

where $Z_r = \sqrt{L_r / (2 \cdot C_j)}$, $\omega_r = \sqrt{1 / (2 \cdot C_j \cdot L_r)}$.

The duration of the stage 6 is:

$$t_6 - t_5 = (\arcsin \frac{V_{in} \cdot n}{2 \cdot I_o \cdot Z_r}) / \omega_r \quad (10)$$

$$i_p(t_6) = \frac{I_o}{n} \cdot \cos \omega_r(t_6 - t_5) \quad (11)$$

Stage 7 [$t_6 - t_7$]: At t_6 , V_{c2} increases to $V_{in}/2$; V_{c3} decreases to 0 V; V_{ab} decreases to $-V_{in}/2$. Then D_3 conducts, which clamps the voltage of S_3 at 0 V, so S_3 can be turned on with zero-voltage. Because D_{r1} , D_{r2} , D_{r3} , and D_{r4} keep conducting, $-V_{in}/2$ is fully applied on L_r , so i_p decays linearly:

$$i_p(t) = i_p(t_6) - \frac{V_{in}}{2 \cdot L_r}(t - t_6) \quad (12)$$

At t_7 , the primary current of transformer is

$$i_p(t_7) = i_p(t_6) - \frac{V_{in}}{2 \cdot L_r}(t_7 - t_6) \quad (13)$$

Stage 8 [$t_7 - t_8$]: At t_7 , S_7 is turned off, C_7 is charged and C_6 is discharged; V_{ab} changes from $-V_{in}/2$ to $-V_{in}$. During this stage, i_p continues to decrease and D_{r1} , D_{r2} , D_{r3} , and D_{r4} remain conducting, which clamps both the primary and secondary voltage at 0 V. During this stage, L_r resonates with C_6 and C_7 , so the voltages on C_6 and C_7 can be given by

$$i_p(t) = i_p(t_7) \cdot \cos \omega_r(t - t_7) \quad (14)$$

$$V_{c7}(t) = i_p(t_7) \cdot Z_r \cdot \sin \omega_r(t - t_7) \quad (15)$$

$$V_{c6}(t) = \frac{V_{in}}{2} - i_p(t_7) \cdot Z_r \cdot \sin \omega_r(t - t_7) \quad (16)$$

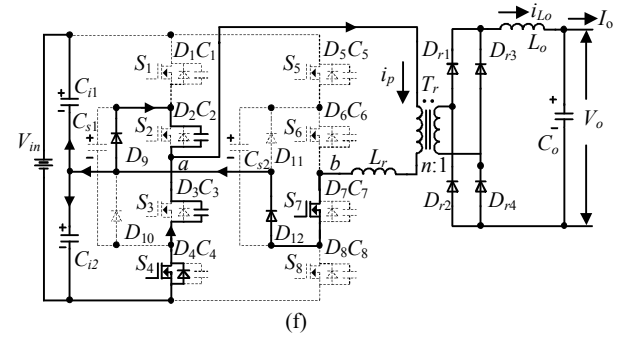
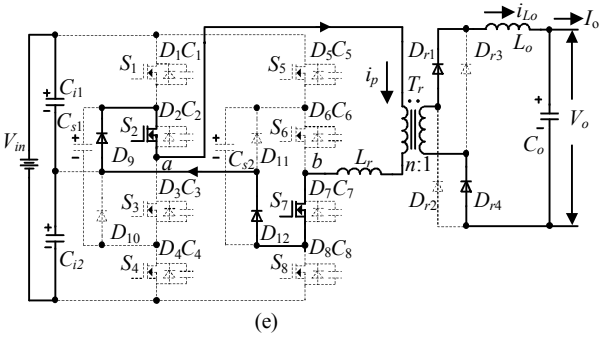
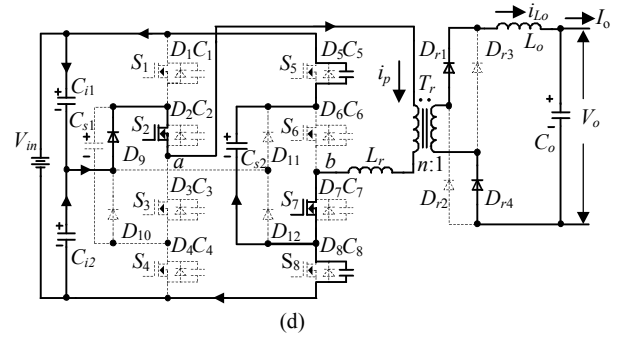
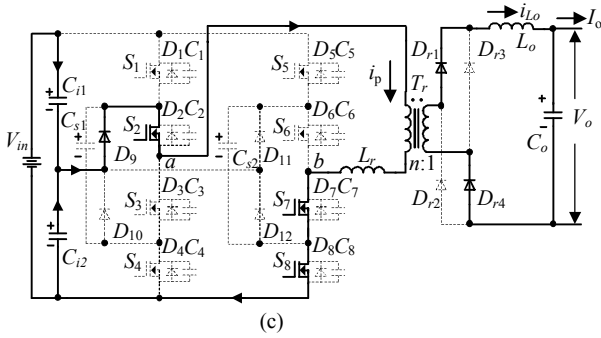
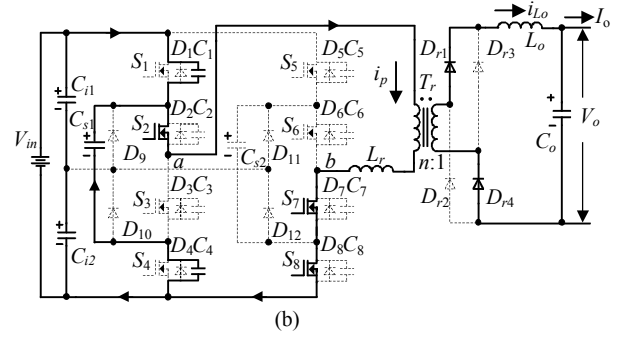
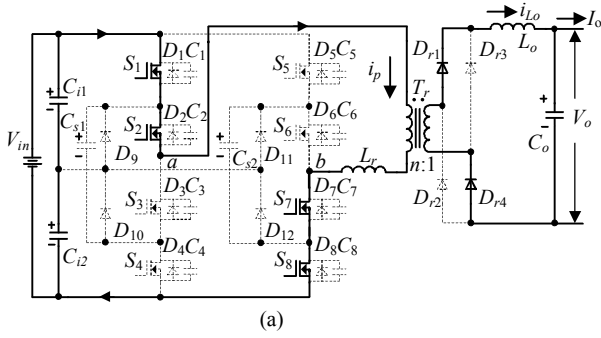
Stage 9 [$t_8 - t_9$]: At t_8 , the voltage of S_7 is $V_{in}/2$, D_6 conducts, which clamps the voltage of S_6 at 0 V, therefore S_6 can be turned on with zero-voltage. D_{r1} , D_{r2} , D_{r3} , and D_{r4} still keep conducting, thus the voltage on L_r is $-V_{in}$ and i_p decreases linearly:

$$i_p(t) = i_p(t_8) - \frac{V_{in}}{L_r}(t - t_8) \quad (17)$$

Stage 10 [$t_9 - t_{10}$]: At t_9 , i_p decreases to 0 A, which means the current direction of i_p would change. The voltage on L_r remains $-V_{in}$, so i_p still decreases linearly.

Stage 11 [$t_{10} - t_{11}$]: At t_{10} , i_p reaches to the negative reflected output current whose value is $-I_o/n$. Then D_{r1} and D_{r4} are turned off, and the input power transfers to load from D_{r2} and D_{r3} .

At t_{11} , S_4 is turned off. The second half cycle [$t_{11} - t_{21}$] starts. The following analysis is similar to the first half cycle [$t_1 - t_{11}$], which is not repeated here.



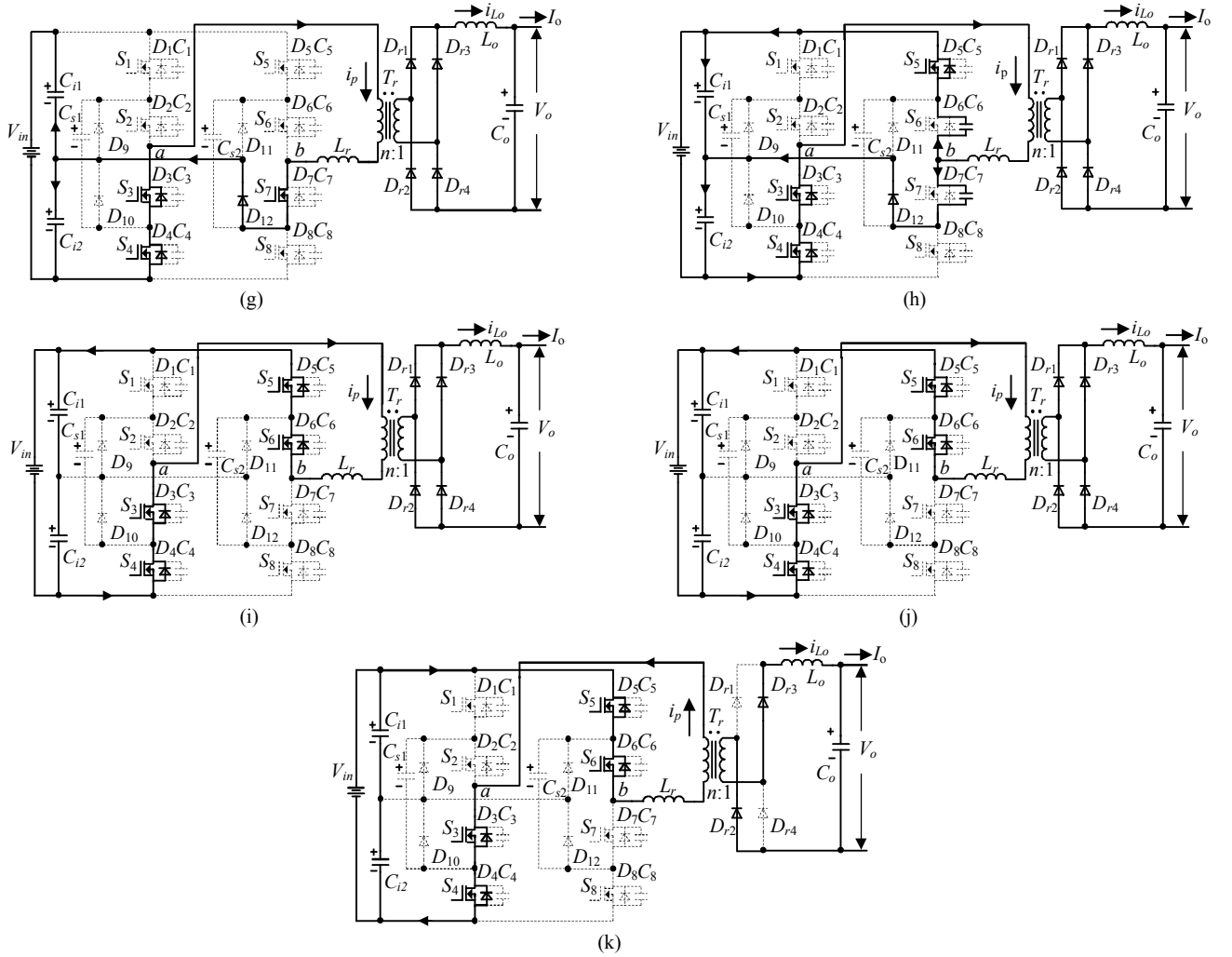


Fig. 2. Equivalent circuits. (a) $[t_0-t_1]$. (b) $[t_1-t_2]$. (c) $[t_2-t_3]$. (d) $[t_3-t_4]$. (e) $[t_4-t_5]$. (f) $[t_5-t_6]$. (g) $[t_6-t_7]$. (h) $[t_7-t_8]$. (i) $[t_8-t_9]$. (j) $[t_9-t_{10}]$. (k) $[t_{10}-t_{11}]$

III. CHARACTERISTIC AND PERFORMANCES

In this section, the characteristic and performances of the FBTL dc/dc converter under the proposed control strategy are analyzed in detail.

A. Voltage Stress of Power Switches

From the above analysis, all the power switches of the FBTL converter only need to withstand half of the input voltage.

B. Duty Cycle Loss

$[t_5 - t_{10}]$ and $[t_{15} - t_{20}]$ are time intervals of duty cycle losses as shown in Fig. 1(b), in which the primary current of the transformer i_p changes from the positive (or negative) direction to the negative (or positive) reflected output filter inductor current. The two time intervals are the same and can be given by

$$t_{10} - t_5 = t_{20} - t_{15} = \frac{\alpha_2}{2} + \frac{2 \cdot L_r \cdot I_o}{n \cdot V_{in}} \quad (18)$$

According to (18), the duty cycle loss in one switching cycle namely D_{loss} can be calculated by

$$D_{loss} = \frac{(t_{10} - t_5) + (t_{20} - t_{15})}{T_s} = \frac{\alpha_2}{T_s} + \frac{4 \cdot L_r \cdot I_o}{n \cdot V_{in} \cdot T_s} \quad (19)$$

C. Conditions of ZVS Achievement for Power Switches

1) Leading Switches

The zero-voltage switch-on of the leading switches S_1 , S_4 , S_5 , and S_8 are mainly decided by the reflected current from the output filter inductance. Normally, the output filter inductance is quite large enough to let the leading switches achieve zero-voltage switch-on even at light load. For instance, in order to ensure the zero-voltage switch-on of the leading switch S_4 , the energy E_1 is needed to fully discharge the parasitic capacitor C_4 and charge the intrinsic capacitor C_1 . The expression of E_1 can be given by

$$E_1 \geq \frac{1}{2} \cdot C_1 \cdot \left(\frac{V_{in}}{2}\right)^2 + \frac{1}{2} \cdot C_4 \cdot \left(\frac{V_{in}}{2}\right)^2 = \frac{1}{4} \cdot C_j \cdot V_{in}^2 \quad (20)$$

2) Lagging Switches

Only the energy of the leakage inductance (and resonant inductance if adding in the circuit) is used for realizing the zero-voltage switch-on of lagging switches S_2 , S_3 , S_6 , and S_7 . Therefore, in order to achieve the zero-voltage switch-on, the following equation (21) should be satisfied.

$$\frac{1}{2}L_r \cdot \left(\frac{I_o}{n}\right)^2 \geq \frac{1}{2}C_j \cdot V_{in}^2 + \frac{V_{in} \cdot \alpha_2}{2} \cdot \sqrt{\left(\frac{I_o}{n}\right)^2 - \frac{C_j}{2L_r} \cdot V_{in}^2} - \frac{V_{in}^2}{8L_r} \cdot \alpha_2^2 \quad (21)$$

D. Output Characteristic

The output voltage V_o can be calculated by

$$\begin{aligned} V_o &= \frac{V_{in}}{n} \cdot \left(1 - \frac{2 \cdot \alpha_1}{T_s} - D_{loss}\right) + \frac{V_{in}}{2 \cdot n} \cdot \frac{4 \cdot \alpha_2}{T_s} \\ &= \frac{V_{in}}{n} \cdot \left(1 - \frac{2 \cdot \alpha_1}{T_s} + \frac{\alpha_2}{T_s} - \frac{4 \cdot L_r \cdot I_o}{n \cdot V_{in} \cdot T_s}\right) \end{aligned} \quad (22)$$

IV. SIMULATION VERIFICATION

In order to verify the proposed double phase-shift control strategy, a simulation model is built in PLECS, whose parameters are listed in Appendix.

In the simulation model, α_2 is set as $5\mu s$ and the output voltage V_o is controlled by adjusting α_1 . Fig. 3 shows the simulation results including voltages V_{in} , V_{ab} , V_o and currents i_p , i_o under the proposed control strategy. Fig. 4 shows the comparison results between the control strategy in [14] and the proposed control strategy. From Fig. 4, it can be observed that the voltage change rate dv/dt of V_{ab} is effectively reduced by utilizing the proposed double phase-shift control strategy, which means the voltage stress on the transformer is reduced, as marked in Fig. 4(b).

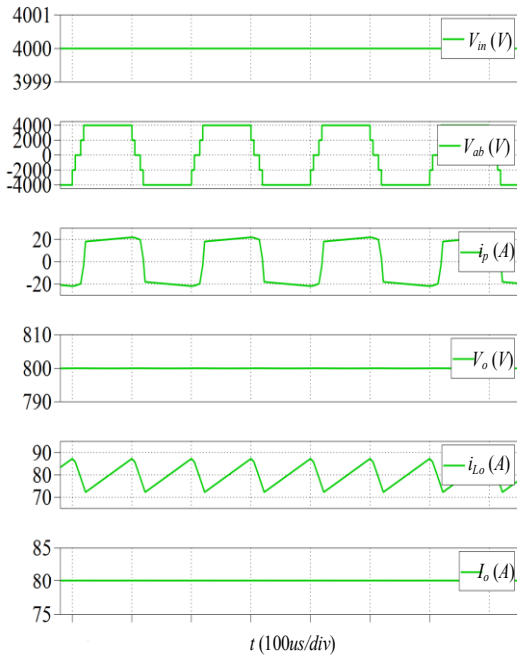
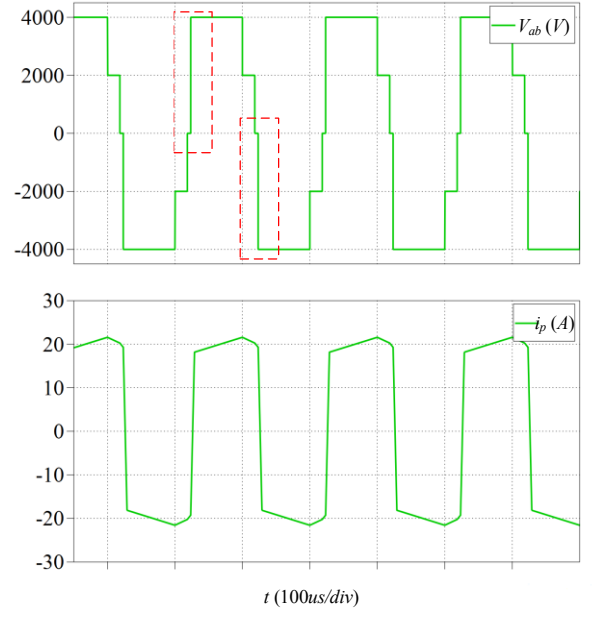
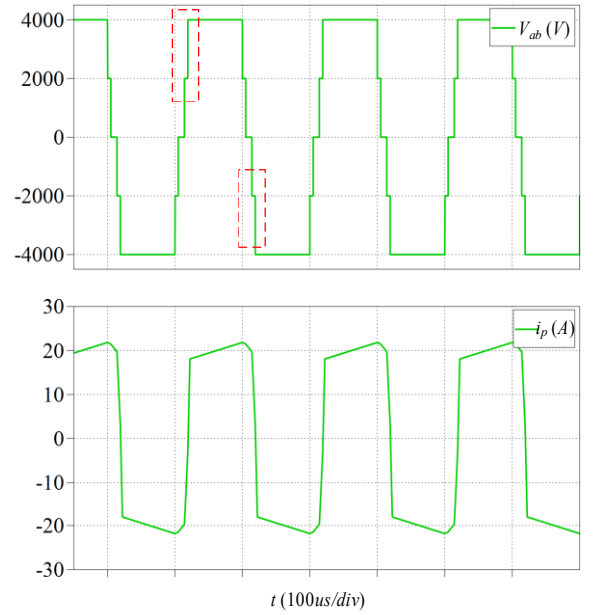


Fig. 3. Simulation results under the proposed control strategy including V_{in} , V_{ab} , V_o , i_p , i_{Lo} , and I_o .



(a)



(b)

Fig. 4. Comparison results including V_{ab} and i_p . (a) Under the control strategy in [14]. (b) Under the proposed control strategy.

V. CONCLUSION AND FUTURE WORK

In this paper, a double phase-shift control strategy is proposed for the FBTL dc/dc converter which is applied to dc distribution grids with the high dc bus voltage. By utilizing the proposed double phase-shift control strategy, the voltage change rate dv/dt and voltage stress on the transformer are

effectively reduced, which means the EMI and reliability of the converter can be improved. The operation principle and performance of the FBTL dc/dc converter under the proposed control strategy are analyzed in detail. Finally, a simulation model is built and simulation results validate the effectiveness and feasibility of the proposed control strategy.

APPENDIX

See Table I.

TABLE I. PARAMETERS OF THE SIMULATION MODEL

Component	Description
Turns Ratio of the Transformer $T_r (n : 1)$	4 : 1
Input Capacitors C_1 and C_2 (μF)	4700
Output Filter Inductor L_o (μH)	1000
Output Filter Capacitor C_o (μF)	4700
Input Voltage V_{in} (kV)	4
Output Voltage V_o (V)	800
α_s (μs)	5
Output Power (kW)	64
Switching Frequency (kHz)	5

REFERENCES

- [1] R. S. Balog, W. Weaver, and P. T. Krein, "The Load as an Energy Asset in a Distributed DC Smart Grid Architecture," *IEEE Trans. Smart Grid*, vol. 3, no. 1, pp. 253–260, Mar. 2012.
- [2] H. Mohsenian-Rad, and A. Davoudi, "Towards Building an Optimal Demand Response Framework for DC Distribution Networks," *IEEE Trans. Smart Grid*, vol. 5, no. 5, pp. 2626–2634, Sep. 2014.
- [3] G. F. Reed, B. M. Grainger, A. R. Sparacino, and M. Zhi-Hong, "Ship to grid: Medium-voltage DC concepts in theory and practice," *IEEE Power Energy Mag.*, vol. 10, no. 6, pp. 70–79, Nov. 2012.
- [4] S. Anand and B. G. Fernandes, "Optimal voltage level for DC microgrids," in *Proc. IEEE Conf. Ind. Electron.*, 2010, pp. 3034–3039.
- [5] D. Salomonsson, L. Soder, and A. Sannino, "An adaptive control system for a DC microgrid for data centers," *IEEE Trans. Ind. Appl.*, vol. 44, no. 6, pp. 1910–1917, Nov./Dec. 2008.
- [6] Y. Chen, M. Haj-ahmed, and M. S. Illindala, "An MVDC microgrid for a remote area mine site: Protection, operation and control," in *Proc. IEEE IAS Annu. Meet.*, Oct. 2014, pp. 1–9.
- [7] F. Canales, P. Barbosa, M. Burdio, and F. Lee, "A zero-voltage switching three-level DC/DC converter," in *Proc. 22nd Int. Telecommun. Energy Conf.*, 2000, pp. 512–517.
- [8] F. Canales, P. Barbosa, and F. C. Lee, "A zero-voltage and zero-current switching three-level dc/dc converter," *IEEE Trans. Power Electron.*, vol. 17, no. 6, pp. 898–904, Nov. 2002.
- [9] I. Barbi, R. Gules, R. Redl, and N. O. Sokal, "DC/DC converter: Four switches $V_{pk} = V_{in}/2$, capacitive turn-off snubbing, ZV turn-on," *IEEE Trans. Power Electron.*, vol. 19, no. 4, pp. 918–927, Jul. 2004.
- [10] Y. Shi, and X. Yang, "Wide range soft switching PWM three-level DC-DC converters suitable for industrial applications," *IEEE Trans. Power Electron.*, vol. 29, no. 2, pp. 603–616, Feb. 2014.
- [11] W. Li, S. Zong, F. Liu, H. Yang, X. He, and B. Wu, "Secondary-side phase-shift-controlled ZVS DC/DC converter with wide voltage gain for high input voltage applications," *IEEE Trans. Power Electron.*, vol. 28, no. 11, pp. 5128–5139, Nov. 2013.
- [12] T. T. Sun, H. S. H. Chung, and A. Ioinovici, "A high-voltage DC-DC converter with $V_{in}/3$ —Voltage stress on the primary switches," *IEEE Trans. Power Electron.*, vol. 22, no. 6, pp. 2124–2137, Nov. 2007.
- [13] Z. Zhang and X. Ruan, "Zero-Voltage-Switching PWM full-bridge three-level converter," in *Proc. 4th Int. Power Electron. Motion Control Conf.*, 2004, pp. 1085–1090.
- [14] Z. Zhang and X. Ruan, "A novel double phase-shift control scheme for full-bridge three-level converter," in *Proc. 20th Annu. IEEE Appl. Power Electron. Conf. Expos.*, Mar., 2005, pp. 1240–1245.
- [15] F. Deng and Z. Chen, "Control of improved full-bridge three-level DC/DC converter for wind turbines in a DC grid," *IEEE Trans. Power Electron.*, vol. 28, no. 1, pp. 314–324, Jan. 2013.